Chinese Journal of Natural Medicines

***Artemisia argyi* extract subfraction exerts an antifungal effect against dermatophytes by disrupting mitochondrial morphology and function**

Le CHEN, Yunyun ZHU, Chaowei GUO, Yujie GUO, Lu ZHAO, Yuhuan MIAO, Hongzhi DU, Dahui LIU

Citation: Le CHEN, Yunyun ZHU, Chaowei GUO, Yujie GUO, Lu ZHAO, Yuhuan MIAO, Hongzhi DU, Dahui LIU, *Artemisia argyi* extract subfraction exerts an antifungal effect against dermatophytes by disrupting mitochondrial morphology and function, Chinese Journal of Natural Medicines, 2024, 22(1), 47−61. doi: 10.1016/S1875−5364(24)60561−3.

View online: https://doi.org/10.1016/S1875−5364(24)60561−3

Available online at www.sciencedirect.com
ScienceDirect
Chinese Journal of Natural Medicines 2024, **22**(1): 47-61
doi: 10.1016/S1875-5364(24)60561-3
Chinese Journal of Natural Medicines

•Original article•

Artemisia argyi extract subfraction exerts an antifungal effect against dermatophytes by disrupting mitochondrial morphology and function

CHEN Le[1, 3Δ], ZHU Yunyun[1Δ], GUO Chaowei[1], GUO Yujie[1], ZHAO Lu[1], MIAO Yuhuan[1], DU Hongzhi[1, 2*], LIU Dahui[1*]

[1] *College of Pharmacy, Hubei University of Chinese Medicine, Wuhan 430065, China;*
[2] *National Resource Center for Chinese Materia Medica, China Academy of Chinese Medical Sciences, Beijing 100700, China;*
[3] *College of Pharmacy, Nanjing University of Chinese Medicine, Nanjing 210023, China*

Available online 20 Jan., 2024

[ABSTRACT] *Artemisia argyi* (*A. argyi*), a plant with a longstanding history as a raw material for traditional medicine and functional diets in Asia, has been used traditionally to bathe and soak feet for its disinfectant and itch-relieving properties. Despite its widespread use, scientific evidence validating the antifungal efficacy of *A. argyi* water extract (AAWE) against dermatophytes, particularly *Trichophyton rubrum*, *Trichophyton mentagrophytes*, and *Microsporum gypseum*, remains limited. This study aimed to substantiate the scientific basis of the folkloric use of *A. argyi* by evaluating the antifungal effects and the underlying molecular mechanisms of its active subfraction against dermatophytes. The results indicated that AAWE exhibited excellent antifungal effects against the three aforementioned dermatophyte species. The subfraction AAWE6, isolated using D101 macroporous resin, emerged as the most potent subfraction. The minimum inhibitory concentrations (MICs) of AAWE6 against *T. rubrum*, *M. gypseum*, and *T. mentagrophytes* were 312.5, 312.5, and 625 μg·mL^{-1}, respectively. Transmission electron microscopy (TEM) results and assays of enzymes linked to cell wall integrity and cell membrane function indicated that AAWE6 could penetrate the external protective barrier of *T. rubrum*, creating breaches ("small holes"), and disrupt the internal mitochondrial structure ("granary"). Furthermore, transcriptome data, quantitative real-time PCR (RT-qPCR), and biochemical assays corroborated the severe disruption of mitochondrial function, evidenced by inhibited tricarboxylic acid (TCA) cycle and energy metabolism. Additionally, chemical characterization and molecular docking analyses identified flavonoids, primarily eupatilin (131.16 ± 4.52 mg·g^{-1}) and jaceosidin (4.17 ± 0.18 mg·g^{-1}), as the active components of AAWE6. In conclusion, the subfraction AAWE6 from *A. argyi* exerts antifungal effects against dermatophytes by disrupting mitochondrial morphology and function. This research validates the traditional use of *A. argyi* and provides scientific support for its anti-dermatophytic applications, as recognized in the Chinese patent (No. ZL202111161301.9).

[KEY WORDS] *Artemisia argyi*; Dermatophyte; Antifungal activity; Mitochondrial structure; Mitochondrial function; Transcriptome analysis

[CLC Number] R965 **[Document code]** A **[Article ID]** 2095-6975(2024)01-0047-15

[Received on] 24-Jul.-2023
[Research funding] This work was supported by the National Natural Science Foundation of China (No. 32270391), the Natural Science Foundation of Hubei Province (Nos. 2023AFA032 and 2022CFB391), the Young Qihuang Scholars of the State Administration of Traditional Chinese Medicine, Hubei Province Administration of Traditional Chinese Medicine Research Project (No. ZY2023Z023), the Earmarked Fund for CARS-21 and Key Project at Central Government Level: the Ability Establishment of Sustainable Use for Valuable Chinese Medicine Resources (No. 2060302).
[*]**Corresponding author]** E-mails: dhz3163@hbtcm.edu.cn (DU Hongzhi); liudahui@hbtcm.edu.cn (LIU Dahui)
[Δ]These authors contributed equally to this work.
These authors have no conflict of interest to declare.

Introduction

Dermatophytosis, a prevalent fungal skin condition caused by dermatophytes, commonly affects the head, hands, and feet [1]. This globally widespread disease is especially rampant in tropical and subtropical areas, with a notably high incidence in China. It significantly impacts numerous individuals through its clinical manifestations, which typically include erythematous, blistering, and pustular lesions, accompanied by intense itching and symptom severity varying according to the infection site [2]. *Trichophyton rubrum*, an anthropophilic dermatophyte, is the predominant species isolated from skin infections, accounting for 69.5% of cases [3],

with *Trichophyton mentagrophytes* and *Microsporum gypseum* also being notable contributors [4]. The primary clinical treatments for dermatophytosis are topical imidazole and allylamine antifungals [5]. Despite their significant efficacy, they are accompanied by a high number of side effects and adverse reactions and present carcinogenicity, teratogenicity, and acute toxicity [6]. In addition, the abuse of broad-spectrum, highly effective antibacterial drugs and glucocorticoids has led to increased resistance of dermatophytes, often resulting in recurrent and challenging to treat infections [7]. Consequently, there is an urgent need to explore efficient, low-toxicity alternatives with potent broad-spectrum antifungal activity to effectively manage dermatophyte infections.

China boasts a wealth of medicinal and edible plant resources. Recent studies have highlighted that a wide array of plant-derived secondary metabolites display potent antifungal properties, including compounds like ellagic acid, licochalcone A, magnoflorine, and loureirin A [8-11]. These plant resources are increasingly favored due to their lower incidence of side effects, diverse formulation possibilities, and reduced likelihood of contributing to drug resistance [12]. In light of these advantages, our research is dedicated to identifying plants with strong antibacterial properties, elucidating their active constituents, and understanding their mechanisms of action against dermatophytes.

Artemisia argyi (*A. argyi*), a member of the Compositae family, is widely distributed in Asia, especially in China. *A. argyi* is also valued for its nutritional and functional components, making it a favorable dietary additive. Historically, in ancient China, the buds and leaves of *A. argyi* were harvested around Tomb-Sweeping Day for consumption in various forms, such as infusions and green dumplings, serving as food supplements [13]. Moreover, *A. argyi* is renowned for its diverse biological activities and has found extensive use in traditional practices. As noted in the 2020 edition of the *Chinese Pharmacopoeia*, *A. argyi*'s external application is recommended for eliminating dampness and alleviating itching. Its medicinal use dates back over 400 years, as documented in the *Compendium of Materia Medica*, particularly as a treatment for ringworm. Traditional practices also included placing *A. argyi* in socks to treat beriberi, a dermatophyte foot infection. Contemporary folkloric use in China still incorporates *A. argyi* for preventing and treating skin diseases, such as bathing and soaking feet with its extracts. These records indicate that *A. argyi* water extract (AAWE) may have significant anti-dermatophytic activity, but scientific evidence has been lacking. Modern pharmacological studies show that *A. argyi* is mainly abundant in volatile oils, flavonoids, phenolic acids, terpenes, and other chemical components and presents significant antibacterial and antiviral effects [14]. While most studies have concentrated on the antifungal activity of *A. argyi*'s volatile oil [15, 16], the antifungal activity of its water extract has received less attention. This oversight is notable given the low concentration and high volatility of the essential oil during processing and preparation. Furthermore, the need for effective treatments against major clinical pathogenic fungi is urgent, including *T. rubrum*, *T. mentagrophytes*, and *M. gypseum*. In addition, previous reports have established the safety of *A. argyi* water extract [17]. Therefore, validating the inhibitory activity of AAWE against dermatophytes is imperative to advance its scientific application and utilization.

In this work, we first evaluated the antifungal activity of AAWE and its subfractions (AAWE1−AAWE6) against three main dermatophytes (*T. rubrum*, *T. mentagrophytes*, and *M. gypseum*). Then, ultra-performance liquid chromatography-quadrupole time-of-flight mass spectrometry (UPLC-QTOF-MS) and high-performance liquid chromatography with a diode array detector (HPLC-DAD) assays were performed to characterize the chemical composition of the most active subfraction (AAWE6) from AAWE. Furthermore, the anti-dermatophytic mechanism of AAWE6 was elucidated by physiological and biochemical detection, transcriptome analysis, and key gene validation. The findings were further substantiated using molecular docking techniques, verification of enzymatic key targets, and quantification of metabolites. The innovative and comprehensive nature of our research culminated in the acquisition of a patent license (No. ZL202111161301.9) in 2022. Overall, our research sheds new light on the anti-dermatophytic properties of *A. argyi* and underscores its potential as a therapeutic agent against critical human pathogens.

Materials and Methods

Materials and reagents

A. argyi was provided by Qichun County, Hubei Province, China. The plant specimens (S200711) were deposited in the Traditional Chinese Medicine Resource Center of Hubei University of Chinese Medicine and authenticated by Professor LIU Dahui (one of the authors of this study).

T. rubrum (No. 340195), *T. mentagrophytes* (No. 340405), and *M. gypseum* (No. 340196) were purchased from BeNa Culture Collection (BNCC, China). Terbinafine was supplied by Shanghai Yuanye Bio-Technology Co., Ltd. (Shanghai, China). Column chromatography was performed on a D101 macroporous resin (Donghong Chemical Co., China). Eupatilin, jaceosidin, and casticin were obtained from Chengdu Herbpurity Co., Ltd. (Chengdu, China). MS-grade acetonitrile, methanol, and formic acid were purchased from Merck (Darmstadt, Germany). Other chemicals and solvents of analytical grade were employed as received without additional purification.

Preparation of AAWE and its six subfractions

Plant materials (6.0 kg), *A. argyi* water crude extract (AAWE, 714.2 g), and its six subfractions, aqueous elution portion (AAWE1, 262.9 g), 10% ethanol elution portion (AAWE2, 29.4 g), 20% ethanol elution portion (AAWE3, 45.6 g), 40% ethanol elution portion (AAWE4, 65.2 g), 60% ethanol elution portion (AAWE5, 13.3 g), and 95% ethanol elution portion (AAWE6, 3.9 g), were reported in our previ-

ous studies [18]. Briefly, the air-dried *A. argyi* (6.0 kg) underwent ultrasonic extraction twice using pure water at room temperature. The extract obtained from the ultrasonic extraction was then concentrated using a rotary evaporator at 50 °C, resulting in crude extracts (714.2 g). Then the crude extracts (450.0 g) were subjected to chromatography using D101 macroporous resin and eluted with EtOH/H_2O (0 : 100, 10 : 90, 20 : 80, 40 : 60, 60 : 40, 95 : 5, *V/V*), yielding six subfractions (AAWE1−AAWE6).

Determination of the antifungal activity of AAWE and its six subfractions against three dermatophytes

T. rubrum, *T. mentagrophytes*, and *M. gypseum* were cultured on potato dextrose agar (PDA) medium for 7−10 days, and hyphae were transferred into liquid Sabouraud medium for seven days at 28 °C to prepare suspension solutions (1−5 × 10^5 CFU·mL^{-1}).

The antifungal activity of AAWE and its six subfractions against dermatophytes was determined by the growth rate method, as described in a prior study [19]. AAWE was dissolved in pure water and then added to PDA to prepare drug-containing plates with concentrations of 0, 1.25, 2.5, 5, and 10 mg·mL^{-1}. Under aseptic conditions, three fungal cultures with similar growth rates were selected, and the 5 mm fungus cake was cut and placed in the center of blank control medium (CK), drug-containing medium, and positive drug medium (terbinafine, 5 μg·mL^{-1}). The cultures were incubated in a biochemical incubator at 28 °C, and the hyphal growth diameter was measured when the CK group occupied the whole plate. Similarly, AAWE1−AAWE6 were dissolved in ethanol to prepare a drug-containing medium with a final concentration of 2.5 mg·mL^{-1} for screening the active subfraction. The ethanol content was the same in the blank and drug-containing groups. In addition, the antifungal effects of the highest active subfraction (AAWE6) were evaluated with concentration gradients of 0, 39.06, 78.125, 156.25, 312.5, 625, and 1250 μg·mL^{-1}. Finally, the inhibition rate (IR) was calculated by the following formula: IR (%) = 100 × (D_c − D_s)/(D_c − D_0), where D_c, D_s, and D_0 represent the diameters of the blank control group, extract-treated group, and fungus cake, respectively.

The minimum inhibitory concentrations (MICs) of AAWE6 against three dermatophytes were assayed by the broth microdilution method based on the Clinical and Laboratory Standards Institute (CLSI) M38-A2 [20]. In a 96-well plate, 100 μL of the prepared spore suspension (1−5 × 10^5 CFU·mL^{-1}) was mixed with 100 μL of AAWE6 (concentrations ranging from 0 to 1250 μg·mL^{-1}) in RPMI 1640 (Solarbio, China) medium, with terbinafine (5 μg·mL^{-1}) as a positive control. The negative control group was treated with RPMI 1640 medium. Subsequently, the 96-well plate was placed at 28 °C for 96 h. The MIC was defined as the lowest concentration capable of visually inhibiting 100% of fungal growth by two people. To obtain the minimal fungicidal concentration (MFC), 100 μL of the culture medium was taken from wells showing no visible growth and spread on PDA plates, which were then incubated at 28 °C for 7 d. The MFC was defined as the minimum concentration yielding no more than five colonies or no viable fungal growth. All these assays were replicated in three independent experiments, each performed in triplicate, to ensure the accuracy and reliability of results.

Chemical composition analysis of the highest active subfraction (AAWE6) using UPLC-QTOF-MS and HPLC-DAD

UPLC-QTOF-MS analysis was performed to identify the chemical components of the active subfraction AAWE6 using a Waters Acquity I-Class ultra-performance liquid chromatograph combined with a Xevo G2-XS quadrupole time-of-flight mass spectrometer (Waters, Milford, Massachusetts, USA). The chromatographic column, chromatography, and mass spectrometry conditions used for analysis refer to our previous work [21].

Quantitative analysis of the main chemical components from AAWE6, including eupatilin, jaceosidin, and casticin, was performed by HPLC-DAD (Shimadzu, Japan). The analytical column was an Agilent ZORBAX Eclipse XDB-C_{18} column (250 mm × 4.6 mm, 5 μm). An ordinary solvent system of A) 0.1% (*V/V*) formic acid in water and B) acetonitrile was used. The gradient elution program was set as follows: 0−12 min, 10%−20% B; 12−25 min, 20%−25% B; 25−50 min, 25%−65% B; 50−55 min, 65%−10% B; and 55−60 min, 10% B. The analysis parameters, including the detection wavelength (330 nm), flow rate (0.8 mL·min^{-1}), column temperature (30 °C), and injection volume (10 μL), were carefully controlled for optimal resolution and reproducibility.

Morphological changes in dermatophytes induced by AAWE6

The ultrastructural changes in *T. rubrum* and *M. gypseum* treated with AAWE6 were observed using transmission electron microscopy (TEM). The above spore suspension was added to liquid Sabouraud medium and incubated in a 28 °C constant temperature shaker for 7 d. Then, the spore fluid was treated with AAWE6 for 24 h, centrifuged at 12 000 r·min^{-1} for 10 min at 4 °C, and washed three times with PBS buffer (pH 7.4) to collect the deposits. After a standard series of preparation steps of dehydration, infiltration, embedding, and cutting as described in a previous study [22], fresh hyphal samples treated with AAWE6 (MIC, 2MIC) and untreated (control) samples were selected and prepared for observation by TEM (Talos L120C, Thermo Fisher, USA). In addition, the grayscale of the internal structure of mitochondria was analyzed using ImageJ software, allowing for a relative quantification of the damage by AAWE6 on the mitochondria of the dermatophyte cells.

Estimation of squalene epoxidase, β-(1,3)-D-glucan synthase and chitin synthase activities in T. rubrum treated with AAWE6

We weighed 0.1 g of fungal deposits treated as described above from each group. Each fungal deposit was mixed with 1 mL of extracting solution (PBS, pH 7.4). This mixture was then ground on ice to ensure thorough disrup-

tion of the fungal cells. The ground mixture was centrifuged at 12 000 r·min^{-1} for 10 min to obtain the supernatant for further analysis. The activities of squalene epoxidase, β-(1,3)-D-glucan synthase, and chitin synthase were determined using a quantitative detection kit (Shanghai Fusheng Industrial Co., Ltd.). The enzyme activity in the samples was calculated based on the concentration of the standard substance and the OD value at 450 nm.

Transcriptome analysis and quantitative real-time PCR (RT-qPCR) analysis

The transcriptome analysis was conducted on three biological replicates from both the control and AAWE6-treated groups, which were previously used for ultrastructural studies. The process encompassed the extraction of total RNA, followed by its quantification and qualification. Subsequent steps involved the construction of cDNA libraries, with three each for the control and AAWE6-treated groups. Transcriptome sequencing was executed by Allwegene Tech Co., Ltd. (Beijing, China). The identification of the differentially expressed genes (DEGs) between the control and AAWE6-treated groups was performed in accordance with methodologies described in a previous report [23]. RT-qPCR was conducted using Real Universal Colour PreMix (SYBR Green) in adherence to the manufacturer's instructions (Tiangen, China). The expression levels of the genes were normalized against the expression of β-tubulin [9]. The specific primer sequences utilized for this study are detailed in Table S1.

Screening of key targets and potential antifungal components by molecular docking

Interactions between the chemical components in AAWE6 and key targets were explored by molecular docking analysis. The two-dimensional (2D) structures of the chemical components present in AAWE6 were retrieved from the PubChem database (https://pubchem.ncbi.nlm.nih.gov/). These structures were then converted into Protein Data Bank (PDB) format using Openbabel, a chemical file translation tool. Concurrently, crystal structures of key target proteins, specifically those bound with distinctive ligands and of relatively high resolution, were obtained from the RCSB Protein Data Bank (PDB, http://www.pdb.org/). After that, molecular docking between the compound and target proteins was analyzed using AutoDock Vina software, and the binding energy was calculated. Finally, with a high degree of binding affinity were visualized using PyMOL software.

Measurement of the dehydrogenase activities and the contents of PA and CA in dermatophytes

The method for preparing the sample solution for this measurement was consistent with the procedure used in determining squalene epoxidase activity, as previously described. Specifically, 0.1 g samples from both the control group and the AAWE6-treated group (at MIC and 2MIC concentrations) were pulverized into a homogenate after the addition of 1 mL of extraction solution. The activities of succinate dehydrogenase (SDH) and malate dehydrogenase (MDH), as well as the concentrations of pyruvic acid (PA) and citric acid (CA) in the supernatant, were then quantified using an assay kit provided by Nanjing Jiancheng Bioengineering Institute, China. Additionally, we evaluated the impact of varying treatment durations with AAWE6 (12, 24, 48, and 72 h) on these indices .

Determination of ATP content and ATPase activity

A 0.1 g mycelium sample was made into a 10% homogenate using nine times the volume of boiling water. The samples were boiled for 10 min in a boiling water bath, and the supernatant was collected after centrifugation to determine the ATP content. In the case of ATPase activity, the mycelium samples were extracted with nine times their volume of PBS buffer (pH 7.4) and homogenized in an ice-water bath. The procedures for both ATP content and ATPase activity measurements were conducted following the kit instructions provided by Nanjing Jiancheng Bioengineering Institute (Nanjing, China).

Statistical analysis

Experimental data are presented as the mean ± standard deviation (SD). All figures were generated using GraphPad Prism 8. The difference between the control and the treatment groups was assessed by one-way analysis of variance (ANOVA), and a *P*-value of less than 0.05 indicated a statistically significant difference. All experiments were performed at least in triplicate.

Results

Screening of the most effective subfraction from A. argyi water extract (AAWE) on antifungal activity against three dermatophytes

A. argyi, a plant used both as an herb and a food in Asia for millennia, is known for its antifungal properties. However, its specific effects against dermatophytes had not been previously documented. To evaluate its anti-dermatophytic effect, we first cultured *T. rubrum*, *M. gypseum*, and *T. mentagrophytes*. Various concentrations of AAWE were introduced into the drug-containing medium to cultivate these three dermatophytes. Our findings indicated that AAWE inhibited the growth of all three dermatophytes in a concentration-dependent manner (Fig. 1A). Significantly, at a concentration of 5 mg·mL^{-1}, AAWE exhibited an inhibition rate of over 60% on the mycelia of these dermatophytes, which increased to more than 90% when the concentration was raised to 10 mg·mL^{-1} (Figs. 1B−1D). These results indicate that AAWE has the potential to be developed as a clinical antifungal agent.

To determine the main antifungal active fraction of AAWE, we subjected the extract to fractionation by D101 macroporous resin chromatography using EtOH/H_2O (0%−95%, *V/V*) gradient elution, yielding subfractions AAWE1−AAWE6. The antifungal activities of six subfractions were evaluated using a colony diameter analysis at a concentration of 2.5 mg·mL^{-1} (Fig. S1 in Supporting Information). As shown in Figs. 1E−1G, treatment with AAWE6 significantly reduced the colony diameters of all three derma-

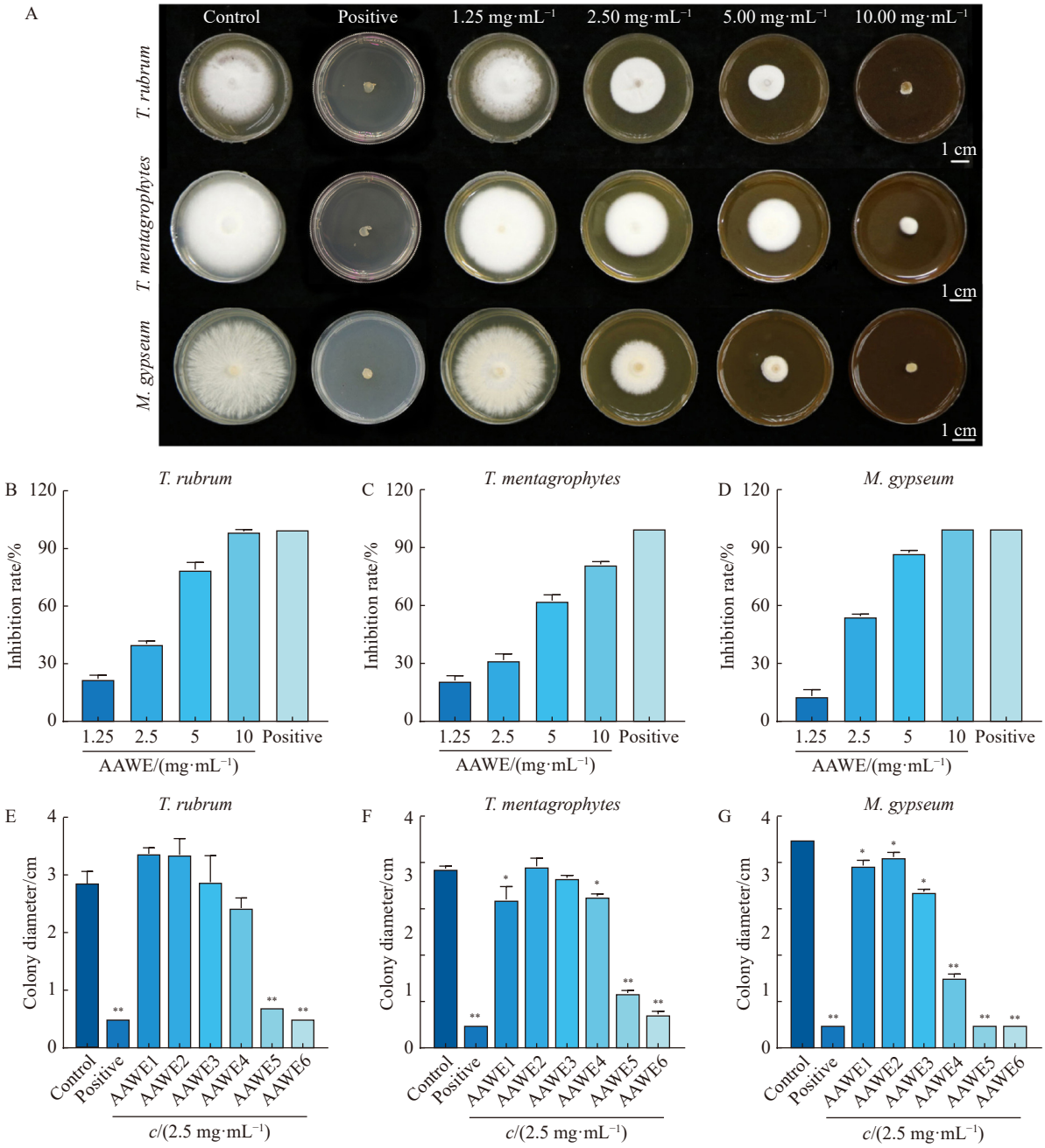

Fig. 1 Antifungal activity of *A. argyi* water extract (AAWE) against *T. rubrum*, *T. mentagrophytes*, and *M. gypseum*, and screening of its active subfractions. (A) Antifungal effect of AAWE on three dermatophytes. (B−D) Inhibition rate (IR) of different concentrations of AAWE (1.25, 2.5, 5, 10 mg·mL^{-1}) on *T. rubrum*, *T. mentagrophytes* and *M. gypseum*, respectively. (E−G) The colony diameters of 6 subfractions isolated by D101 macroporous resin on *T. rubrum*, *T. mentagrophytes* and *M. gypseum*, respectively. Data are presented as the mean ± SD (n = 3), $^{*}P < 0.05$ and $^{**}P < 0.01$ *vs* the control by ANOVA.

tophytes to sizes comparable to their original fungus cake diameters, an effect similar to that observed with terbinafine treatment (P < 0.01). Thus, AAWE6 was identified as the most effective subfraction and selected for further investigation of its anti-dermatophytic effects and molecular mechanisms.

Further studies confirmed AAWE6 as a potent anti-dermatophytic agent. The inhibitory effect of AAWE6 on the dermatophytes intensified with an increase in its concentration (Fig. 2A). Notably, AAWE6 demonstrated a stronger inhibitory effect on *T. rubrum* and *M. gypsum* but a slightly weaker impact on *T. mentagrophytes*. The inhibition rate of AAWE6 exceeded 70% for *T. rubrum* and *M. gypsum* at 625 μg·mL^{-1} (Figs. 2B−2D). More precisely, AAWE6 exhibited lower MIC and MFC values against *T. rubrum* (312.5 μg·mL^{-1} for MIC and 2.5 mg·mL^{-1} for MFC), *M. gypseum* (312.5 μg·mL^{-1} for MIC and 2.5 mg·mL^{-1} for MFC) and *T. mentagrophytes* (625 μg·mL^{-1} for MIC and 5 mg·mL^{-1} for

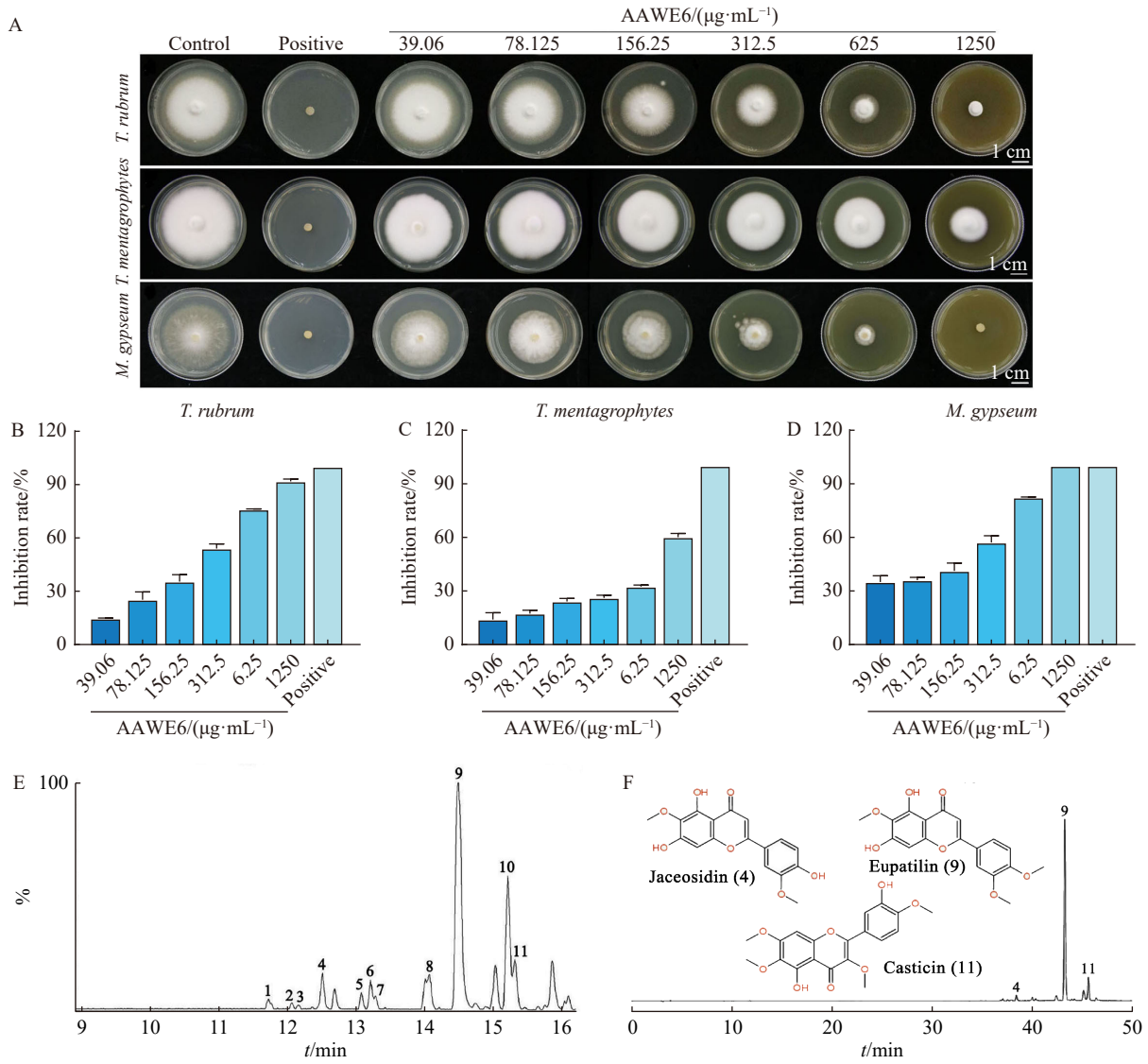

Fig. 2 Antifungal activity of the most effective active subfraction AAWE6 against *T. rubrum*, *T. mentagrophytes* and *M. gypseum*, and its chemical composition analysis using UPLC-QTOF-MS and HPLC-DAD. (A) Antifungal effect of AAWE6 on three dermatophytes. (B−D) IR of different concentrations of AAWE6 (39.06, 78.125, 156.25, 312.5, 625, 1250 μg·mL^{-1}) on *T. rubrum*, *T. mentagrophytes* and *M. gypseum*, respectively. (E) Base peak intensity (BPI) chromatogram in the negative ion mode of AAWE6 by UPLC-QTOF-MS. (F) In the quantitative analysis of AAWE6 using HPLC-DAD, peaks at 4, 9, and 11 represent jaceosidin, eupatilin, and casticin, respectively. Data are presented as the mean ± SD (n = 3).

MFC). When compared with the MICs of other plant extracts/compounds against dermatophytes reported in recent studies, the efficacy of AAWE6 becomes even more evident (Table 1). Therefore, AAWE6 emerges as a promising candidate for the discovery of natural antifungal compounds.

Analysis of the chemical constituents in the most effective subfraction AAWE6 by UPLC-QTOF-MS and HPLC-DAD

In the negative mode, the UPLC-QTOF-MS method was used to clarify the bioactive constitutions of subfraction AAWE6. The base peak intensity (BPI) chromatogram is shown in Fig. 2E. Ion information for eleven compounds was obtained, with peaks 1−9 and 11 identified as flavonoids (Table 2) [27]. These flavonoids are primarily characterized by hydroxyl and oxymethyl group substitutions at various positions and numbers, typically exhibiting $[M - H]^-$ signals and sequential $CH_3\cdot$ removal signals [28]. Collectively, these results showed that flavonoids constitute the main antifungal compounds in AAWE6.

Furthermore, the concentrations of three primary flavonoids in AAWE6 were quantified using HPLC-DAD at 330 nm: jaceosidin (peak 4), eupatilin (peak 9), and casticin (peak 11) (Fig. 2F). Their calibration curves were established as Y_1 = 52 526X + 4218.6 (R^2 = 0.9993) for jaceosidin, Y_2 = 42 143X + 31 366 (R^2 = 0.9996) for eupatilin, along with Y_3 = 34 480X + 20 024 (R^2 = 0.9993) for casticin. Obviously, eupatilin was found to be the most abundant (131.16 ± 4.52 mg·g^{-1}) in AAWE6, followed by casticin (9.87 ± 0.35 mg·g^{-1}) and jaceosidin (4.17 ± 0.18 mg·g^{-1}) in succession.

Table 1 MICs of AAWE6 and potential anti-dermatophytic drugs reported in recent years.

Extracts/Compounds	MIC/(μg·mL^{-1})			
	T. rubrum	*M. gypseum*	*T. mentagrophytes*	References
AAWE6	312.5	312.5	625.0	–
Ethanol extracts of *Dryopteris fragrans*	59.0–1890.0	≥ 236.0	≥ 236.0	[24]
Essential oil from *Piper ecuadorense*	62.5	–	62.5	[25]
Oxyresveratrol from *Morus alb*	500.0	–	–	[26]
Matrine from *Sophora flavescens*	780.0	–	–	[4]

Table 2 Identification of chemical components in the active fraction (AAWE6).

No.	t_R/min	$[M-H]^-$	Molecular formula	MS/MS	Proposed compound
1	11.82	269.0472	$C_{15}H_{10}O_5$	151.0003, 117.0337	Apigenin
2	12.17	299.0579	$C_{16}H_{12}O_6$	285.0390, 284.0293, 256.0293, 227.0297	Hispidulin
3	12.28	359.0791	$C_{18}H_{16}O_6$	344.0541, 329.0627, 314.0058, 301.0362	Centaureidin
4	12.63	329.0691	$C_{17}H_{14}O_7$	314.0433, 299.0214, 145.0292	Jaceosidin
5	13.22	359.0791	$C_{18}H_{16}O_8$	344.0541, 329.0308, 314.0058, 301.0340, 133.0297	5,6,4'-Trihydroxy-7,8,3'-trimethoxyflavone
6	13.36	359.0725	$C_{18}H_{16}O_8$	313.0706, 298.0419, 283.0214, 152.0535, 117.0375	Irigenin
7	13.43	359.0791	$C_{18}H_{16}O_8$	344.0541	Eupatin
8	14.25	313.0706	$C_{17}H_{14}O_6$	298.0480, 283.0214, 152.0492, 117.0337	Cirsimaritin
9	14.68	343.0817	$C_{18}H_{16}O_7$	328.0607, 313.0333, 298.0115, 132.0204	Eupatilin
10	15.43	283.0569	$C_{16}H_{12}O_5$	268.0375, 239.0363, 211.0398, 183.0437, 151.0003, 117.0337	Physcion
11	15.54	373.0911	$C_{19}H_{18}O_8$	358.0657, 343.0426, 328.0225, 257.0049, 229.0128, 201.0186, 173.0238, 145.0292, 117.0337	Casticin

Moreover, these flavonoids were predominantly concentrated in AAWE6, with minimal presence in other subfractions (Fig. S2), underscoring their significance in the antifungal efficacy of AAWE6.

AAWE6-induced damage to the mitochondrial morphology of dermatophytes

Having established the antifungal activity of AAWE6, we proceeded to investigate its underlying mechanism to provide further scientific support for its development and application. TEM images revealed clear morphological alterations and structural damage of *T. rubrum* cells induced by AAWE6 treatment, which were mainly manifested by disintegration of the cell wall and membrane and disruption of the internal structure of mitochondria. In the control group, *T. rubrum* cells maintained structural integrity with clearly visible internal mitochondria (Fig. 3A). However, in the AAWE6-treated group, notable changes were observed: the cytoplasm appeared shrunken, detached from the cytoderm, and the internal structure of mitochondria was compromised with indistinct cristae (Figs. 3B and 3C). More precisely, the relative grayscale of mitochondria in *T. rubrum* treated with AAWE6 decreased significantly (Fig. 3D). Additionally, there was a marked reduction in glycogen granules and an increase in autophagosomes post-AAWE6 treatment. Similar microstructural damages were also observed in *M. gypseum* cells treated with AAWE6 (Fig. S3). These results demonstrate that AAWE6 can penetrate the protective barrier of the fungus, causing substantial disruption to critical sites of energy metabolism.

AAWE6-induced disruption of the cell wall and cell membrane of dermatophytes

In the realm of fungal biology, *β*-(1,3)-D-glucan synthase and chitin synthase are recognized as crucial enzymes for maintaining cell wall integrity, facilitating the production of *β*-1,3-glucan and chitin, respectively [10, 29]. To assess the impact of AAWE6 on the cell wall integrity of *T. rubrum*, we measured the activities of these key enzymes following treatment with AAWE6 at MIC and 2MIC concentrations. The

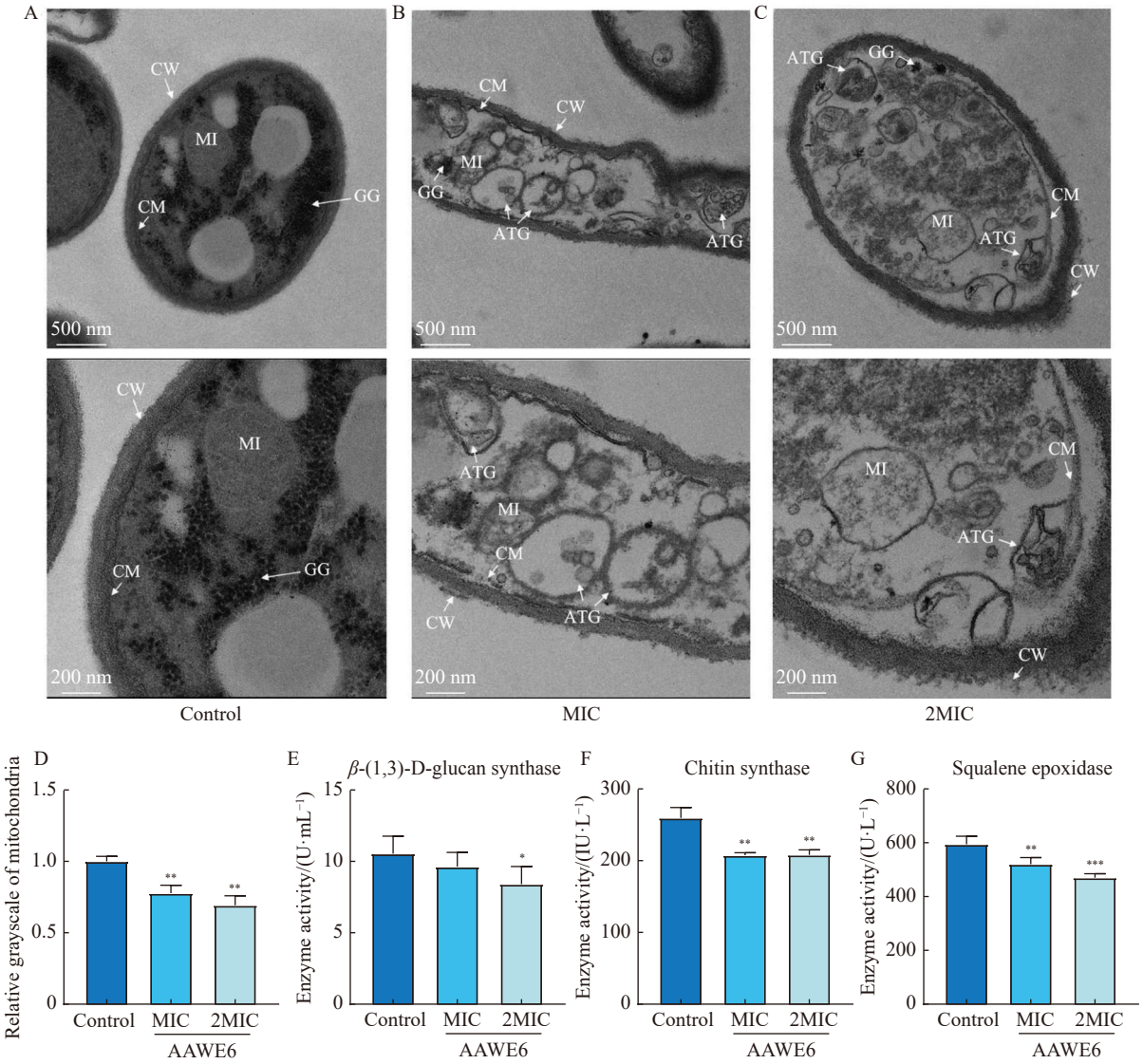

Fig. 3 Disruption of *T. rubrum* cell wall integrity, cell membrane function, and ultrastructure treated with AAWE6 (MIC, 2MIC). (A−C) The ultramicroscopic structures under transmission electron microscopy (TEM) in the control group, MIC group, and 2MIC group, respectively. CW, cell wall; CM, cell membrane; MI, mitochondria; GG, glycogen granule; ATG, autophagosome. (D) The grayscale of the internal structure of mitochondria. (E−G) The inhibitory effects of AAWE6 on *β*-(1,3)-D-glucan synthase, chitin synthase, and squalene epoxidase activities, respectively. The data are presented as the mean ± SD (n = 3), $^{*}P$ < 0.05, $^{**}P$ < 0.01 and $^{***}P$ < 0.001 *vs* the control by ANOVA.

findings revealed a significant reduction in the activities of both *β*-(1,3)-D-glucan synthase and chitin synthase in the presence of AAWE6 (P < 0.05 or P < 0.01) (Figs. 3E and 3F). Moreover, the effect of AAWE6 on the cell membrane function of *T. rubrum* was evaluated by measuring squalene epoxidase activity. As depicted in Fig. 3G, squalene epoxidase activity exhibited a dose-dependent decrease with increasing concentrations of AAWE6. Collectively, these results indicate that AAWE6's antifungal action is mediated through the disruption of both the cell wall and cell membrane integrity of *T. rubrum*.

Transcriptome analysis of differentially expressed genes in T. rubrum treated with AAWE6

Transcriptomics offers a comprehensive and objective way to examine gene expression changes following drug treatment, making it a valuable tool for elucidating drug action mechanisms. In our study, we employed transcriptome analysis to unravel the molecular mechanism behind the antifungal efficacy of AAWE6 against dermatophytes. This analysis involved comparing *T. rubrum* samples from the control group with those treated with AAWE6 at the MIC level. We identified significant changes in gene expression: a total of 2018 differentially expressed genes (DEGs) were upregulated, and 1918 DEGs were downregulated, applying $|\log_2(\text{fold change})| \geq 1$ and a Q-value (the corrected P value) < 0.05 as the screening criteria (Fig. 4A). Kyoto Encyclopedia of Genes and Genomes (KEGG) pathway enrichment analysis of these DEGs revealed that the upregulated genes predom-

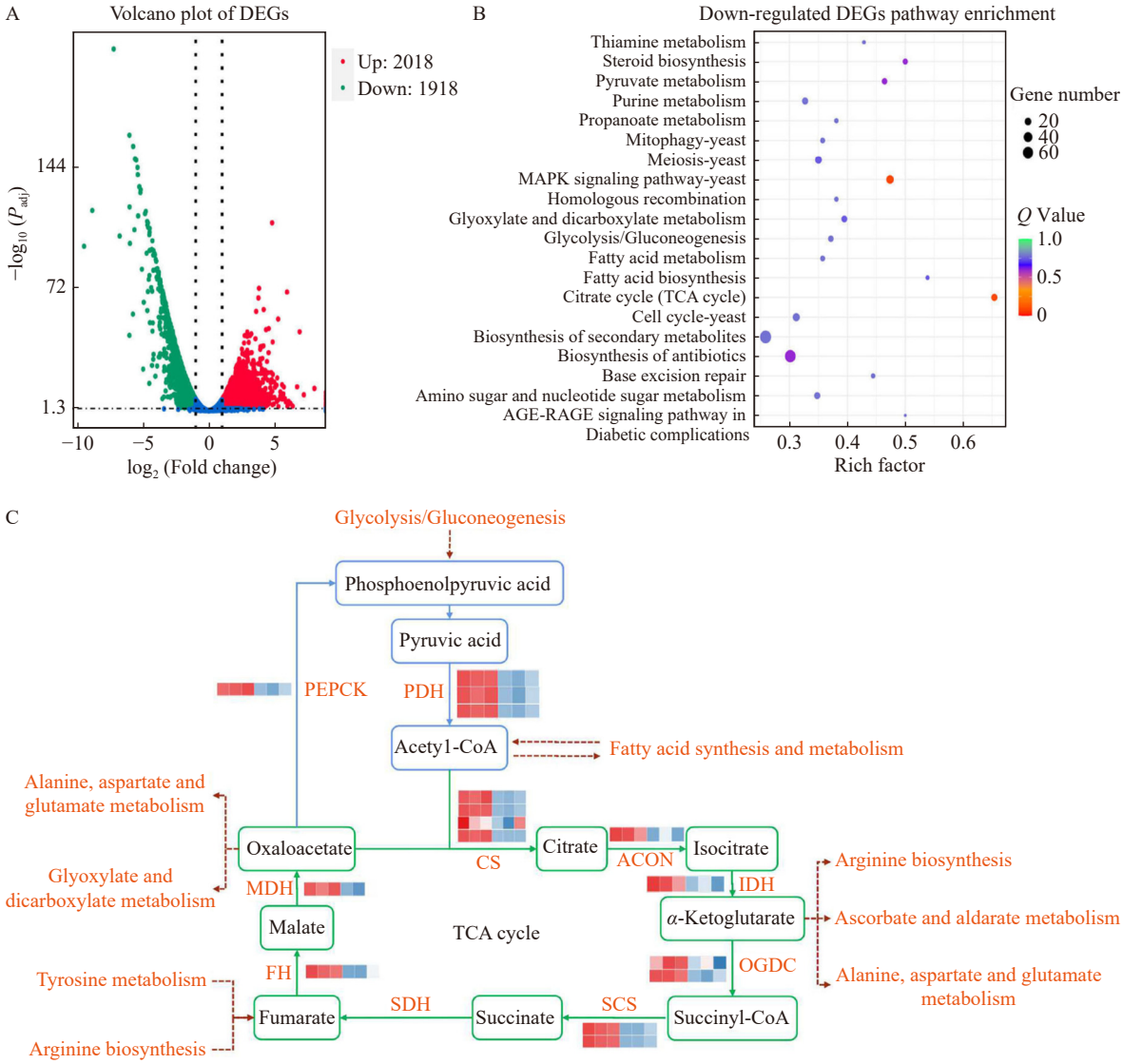

Fig. 4 Transcriptome analysis of *T. rubrum* between the control group and AAWE6-treated group (MIC). (A) 2018 DEGs were upregulated, and 1918 DEGs were downregulated in the volcano plot. (B) KEGG enrichment analysis of downregulated DEGs with TCA cycle as the most significant pathway. (C) The overall distribution of the 16 downregulated DEGs in the TCA cycle pathway.

inantly concentrated in pathways related to the peroxisome, ABC transporters, and glutathione metabolism (Fig. S4). This result indicated that *T. rubrum* might experience oxidative stress following exposure to AAWE6. Conversely, downregulated DEGs showed significant enrichment in pathways such as the citric acid (TCA) cycle, fatty acid biosynthesis and metabolism, glycolysis/gluconeogenesis, and amino sugar and nucleotide sugar metabolism (Fig. 4B).

As shown in Fig. 4C, there were 16 DEGs involved in the TCA cycle. All of these genes were downregulated and were distributed in almost all major processes in the pathway. The synthesis of several key metabolites, including phosphoenolpyruvic acid, acetyl-CoA, α-ketoglutaric acid, and oxaloacetate, was notably inhibited. These metabolites are not only integral to the TCA cycle but also serve as crucial links in carbohydrate, lipid, and amino acid metabolism. In summary, our findings suggest that AAWE6 exerts its antidermatophytic effects primarily by inhibiting the TCA cycle involved in respiratory metabolism, subsequently impacting the overall nutrient metabolism of the organism.

Validation of key genes in the TCA cycle pathway by RT-qPCR

Following the transcriptome analysis, we generated an expression heatmap for 16 DEGs associated with the TCA cycle pathway (Fig. 5A). To validate the reliability of the transcriptome data, we selected eight of these DEGs for further analysis using RT-qPCR, including *TERG_08639* (encoding phosphoenolpyruvate carboxykinase, PEPCK), *TERG_06560* (encoding pyruvate dehydrogenase, PDH), *TERG_04125* (encoding citrate synthase, CS), *TERG_07814* (encoding isocitrate dehydrogenase, IDH), *TERG_02628* (encoding 2-oxoglutarate dehydrogenase, OGDC), *TERG_04056*

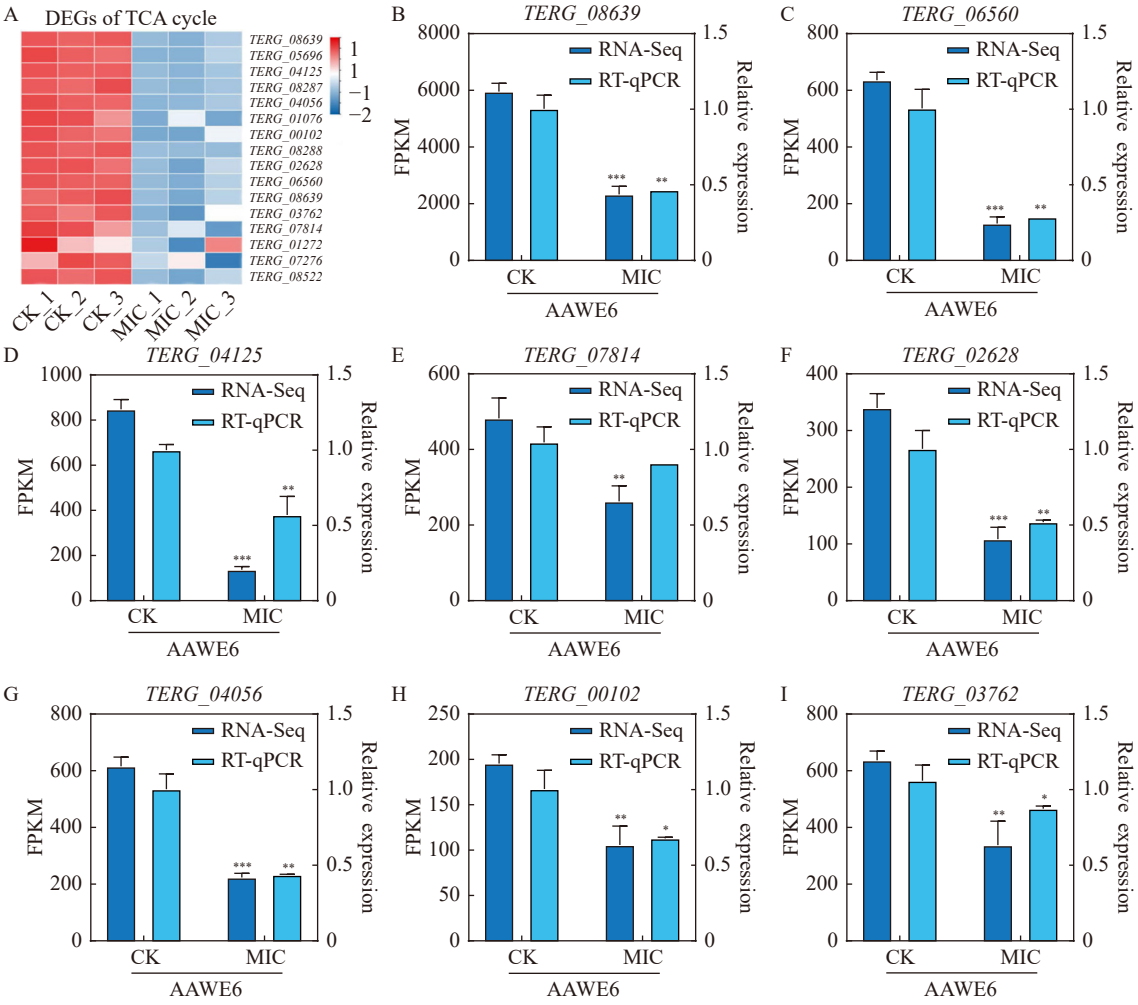

Fig. 5 Comparative analysis of transcriptome results and quantitative real-time PCR (RT-qPCR) data. (A) The expression heatmap of 16 DEGs related to the TCA cycle pathway in each sequencing sample. (B−I) Comparative analysis of the expression and transcriptome sequencing results of eight genes, and they encode PEPCK, PDH, CS, isocitrate dehydrogenase (IDH), 2-oxoglutarate dehydrogenase (OGDC), succinyl-CoA synthetase (SCS), fumarate hydratase (FH) and malate dehydrogenase (MDH), respectively. The data are presented as the mean ± SD (n = 3), $^{*}P < 0.05$, $^{**}P < 0.01$ and $^{***}P < 0.001$ *vs* the control by ANOVA.

(encoding succinyl-CoA synthetase, SCS), *TERG_00102* (encoding fumarate hydratase, FH), and *TERG_03762* (encoding malate dehydrogenase, MDH). The results were consistent with the transcriptome (Figs. 5B−5I), indicating that AAWE6 significantly inhibits the TCA cycle of *T. rubrum*.

Identification of key targets and potential antifungal components using molecular docking

Building on the findings that enzymes like PDH, CS, IDH, SDH, and MDH involved in the TCA cycle may be pivotal targets of AAWE6's antifungal activity, we proceeded to identify key targets and potential antifungal components within AAWE6 through molecular docking. This involved examining the binding affinity of 11 compounds present in AAWE6 to the five aforementioned proteins. By calculating the binding energy, we found that the binding energies of 11 compounds to MDH and SDH were lower, among which jaceosidin and eupatilin were particularly prominent (Fig. 6A). These results suggest that MDH and SDH are likely key targets for the antifungal action of AAWE6, and jaceosidin and eupatilin are the principal antifungal components within the extract. Therefore, we further explored the preferred binding sites of jaceosidin and eupatilin to two key targets.

Since jaceosidin and eupatilin differ only one CH_3· group in structure, they were highly similar to the binding sites of the same target. As shown in Fig. 6B, the two methoxy groups and the hydroxyl groups at positions 4' and 7 of jaceosidin could generate hydrogen bonds with ARG80, GLY12, HIS187, and VAL13 in MDH. In addition to two methoxy groups, the hydroxyl group at positions 5 and 7 and the carbonyl group at position 4 of eupatilin formed six hydrogen bonds with MDH in ARG80, GLY12, HIS187 and ILE116 (Fig. 6C). In the process of interaction between two compounds and SDH, they all produced five hydrogen bonds through three oxygen atoms and one atom (Figs. 6D and 6E). The difference was that the hydrogen atom of jaceosidin was

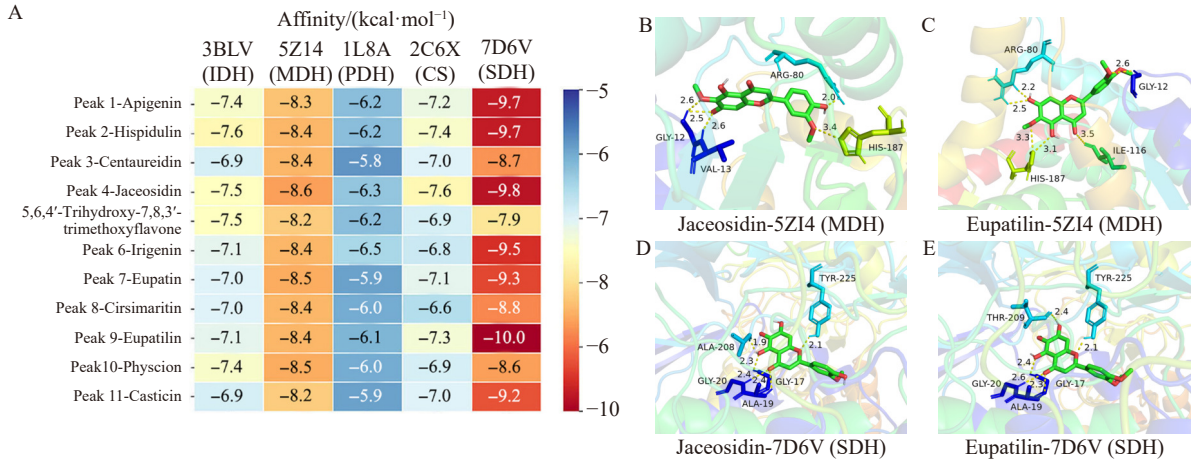

Fig. 6 Molecular docking to explore potential antifungal components in AAWE6. (A) Binding energy heatmap for molecular docking of 11 compounds from AAWE6 and five important targets in the TCA cycle. (B and C) The preferred docking position and interactions of jaceosidin and eupatilin with MDH, respectively. (D and E) The preferred docking position and interactions of jaceosidin and eupatilin with SDH, respectively.

on 5-OH, while that of eupatilin was on 7-OH. They shared four of the five binding sites with the SDH protein. According to the above results, MDH and SDH may be the key targets for AAWE6 to exert antifungal effects, and jaceosidin and eupatilin have excellent direct binding ability with them.

Effects of AAWE6 on mitochondrial function of dermatophytes

Effects of AAWE6 on key enzymes and metabolites related to the TCA cycle

SDH and MDH are two important oxidoreductases in the TCA cycle [30] that also represent potential key targets in this study. Therefore, we examined the effect of different concentrations of AAWE6 on SDH and MDH activity of *T. rubrum*. After AAWE6 treatment, SDH activity increased by 2.1 times at the MIC concentration and decreased by 45.6% at the 2MIC concentration (Fig. 7A). The MDH activity after MIC and 2MIC treatment was 92.7% and 10.2% of that of the untreated group, respectively (Fig. 7B). Moreover, AAWE6 inhibited the concentrations of PA and CA in *T. rubrum*, which are two key organic acids in aerobic respiration, in a concentration-dependent manner (Figs. 7C and 7D). In addition, MDH activity and PA content in *M. gypsum* were also significantly inhibited by AAWE6 treatment (Fig. S3). These results fully suggested that AAWE6 seriously disrupted the process of the TCA cycle of dermatophytes. To identify the key regulatory protein targets, we also investigated the temporal effects of AAWE6 on SDH, MDH, PA, and CA in *T. rubrum* (Fig. S5). It was found that MDH activity exhibited the most significant time dependence.

Effects of AAWE6 on ATP content and ATPase activity

ATP synthesis is an equally important part of mitochondrial biochemical reactions, and its content directly affects the normal energy metabolism of fungi [31]. Figs. 7E and 7F show the effects of AAWE treatment on the ATP content and ATPase activity in *T. rubrum*, respectively. Compared with the control group, the ATP content in the AAWE6-treated groups decreased by more than 70% with increasing exposure concentration. When exposed to the MIC and 2MIC concentrations of AAWE6, ATPase activities decreased by 32.8% and 39.1%, respectively, in *T. rubrum*. In short, AAWE6 hinders the energy generation and consumption in the mitochondria of *T. rubrum*.

Discussion

As a common medicinal and edible plant used to prevent and treat skin diseases, *A. argyi* has been known for its antifungal properties, primarily attributed to its essential oil. However, the antifungal effectiveness of its water extract (AAWE), which aligns with its classic application, has not been scientifically validated until now. In this study, we focused on exploring the antifungal effects of AAWE on three key dermatophytes and established that the subfraction AAWE6, isolated using D101 macroporous resin, was the most effective component (Fig. 8). Considering the efficacy and clinical importance, *T. rubrum* was mainly used for further mechanistic studies. Subsequently, physiological, biochemical, and transcriptome analysis revealed the subfraction AAWE6 from *A. argyi* exerted antifungal effects against *T. rubrum* by disrupting mitochondrial morphology and function. Moreover, qualitative and quantitative analyses of the chemical composition from AAWE6 and molecular docking with key targets elucidated the potential antifungal components. Briefly, this study presents the first report on the anti-dermatophytic effect of *A. argyi* extract, which ensures that we are granted patents in China (No. ZL202111161301.9). Importantly, it provides scientific evidence supporting the development of clinical antifungal agents.

It is reported that the water extract of *A. argyi* can inhibit the growth of common microbial strains, such as *Staphylococcus aureus*, *Escherichia coli*, and *Bacillus subtilis* [14]. However, there is no scientific report on the prevention and treatment of dermatophyte infections with *A. argyi* extract. In

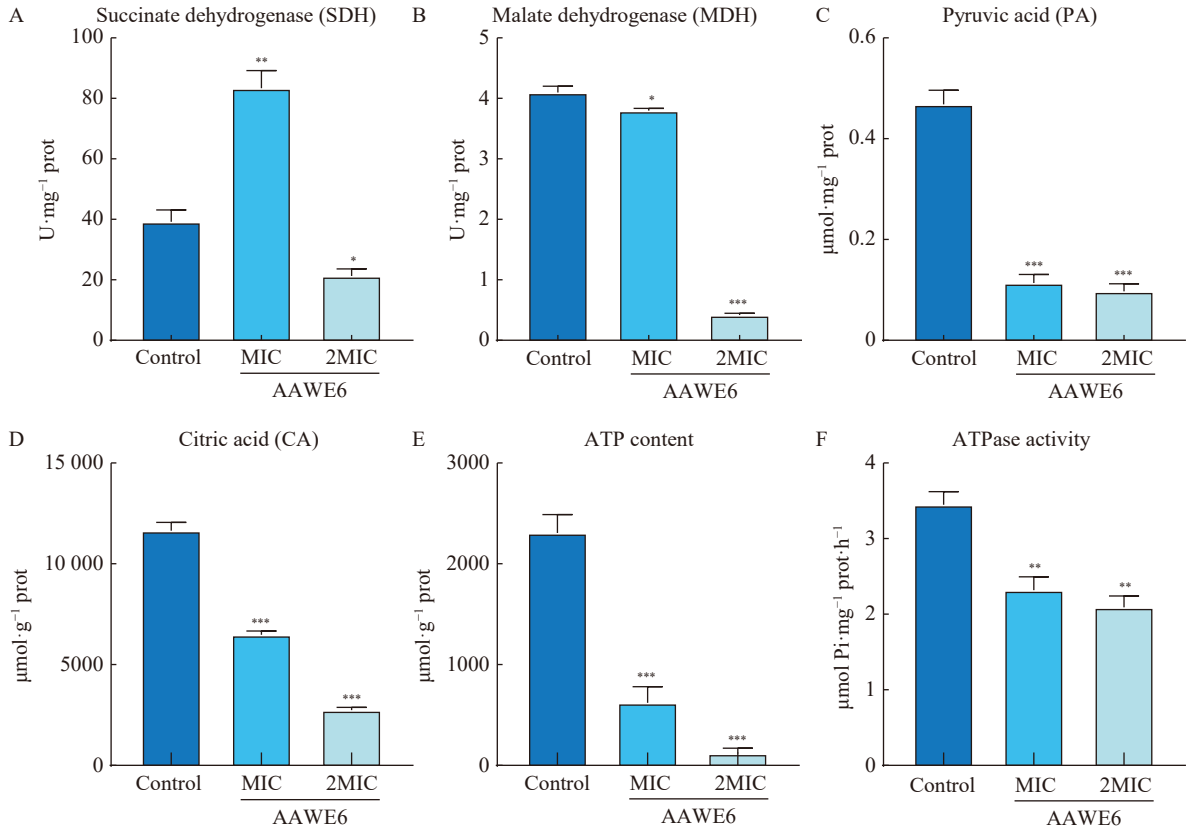

Fig. 7 Determination of several enzyme activities and metabolite contents of *T. rubrum* closely related to the TCA cycle after AAWE6 treatment. (A)The activity of succinate dehydrogenase (SDH). (B) The activity of malate dehydrogenase (MDH). (C) The content of pyruvic acid (PA). (D) The content of citric acid (CA). (E) The content of ATP. (F) The activity of ATPase. The data are presented as the mean ± SD (n = 3), $^{*}P < 0.05$, $^{**}P < 0.01$ and $^{***}P < 0.001$ *vs* the control by ANOVA.

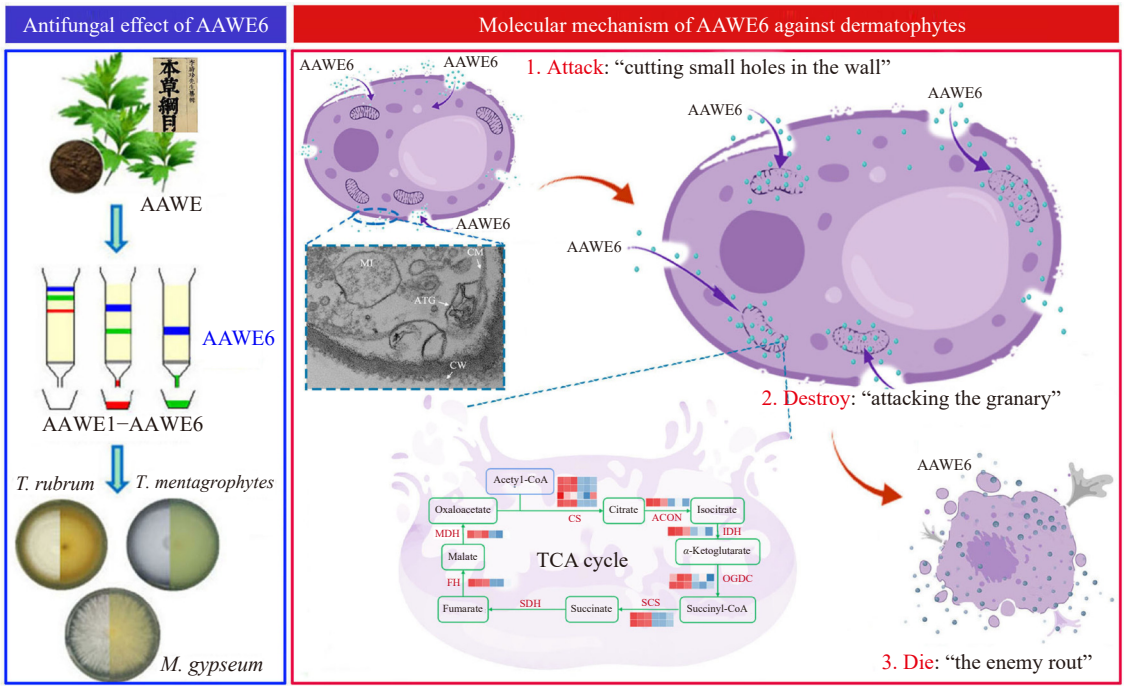

Fig. 8 Schematic diagram of screening the most effective subfraction (AAWE6) against dermatophytes and exploring its molecular mechanisms of *A. argyi*.

addition, folk practices often use *A. argyi* to soak feet or fumigate to disinfect and relieve itching, but also without scientific evidence. In this study, the MIC of the most effective subfraction AAWE6 (MIC 312.5 μg·mL^{-1} for *T. rubrum*) was significantly lower than that of traditional Chinese medicine extracts and monomer components in our study that have been widely reported (Table 1), such as matrine (MIC 780 μg·mL^{-1}) from *Sophora flavescens* [4] and oxyresveratrol (500 μg·mL^{-1}) from *Morus alba* [26]. Given its remarkable efficacy (Figs. 1 and 2), our systematic research strongly supports the further application of *A. argyi* extract, particularly the AAWE6 subfraction, in antifungal treatments. In addition, it also offers a new idea for *A. argyi* as a health-promoting food ingredient to prevent human pathogens.

Understanding the molecular mechanism of a drug is crucial for its effective application. The fungal cell wall and membrane serve as vital protective barriers against external osmotic shocks [32]. Our study revealed that the presence of AAWE6 led to reduced activities of *β*-(1,3)-D-glucan synthase, chitin synthase, and squalene epoxidase. This finding aligns with the observed structural damage to the cell wall and cell membrane of *T. rubrum*, as seen in TEM images (Fig. 3). While AAWE6 exhibited a significant inhibitory effect, its mechanism appears distinct from that of traditional antifungal drugs like terbinafine and ketoconazole [33]. Importantly, the structural damage to the cell wall and membrane caused by AAWE6 facilitates the entry of the drug, thereby enhancing its effectiveness. One of the most pronounced effects of AAWE6 is the disintegration of mitochondrial internal structures. Autophagy involves the formation of a bilayer membrane structure in the cytoplasm that engulfs damaged material and transports it to lysosomes for degradation [34]. The increase in autophagosomes also reflected the damaged state of cells. In addition, the decrease in glycogen granules indicated that glucose metabolism in *T. rubrum* cells was inhibited. In summary, our study posits that AAWE6 exerts its antifungal effects by initially creating “small holes” in the cell wall and membrane. This breach allows AAWE6 to affect the structure and function of mitochondria (“the granary”) severely. Ultimately, these combined effects lead to cellular collapse and the effective inhibition of *T. rubrum* (Fig. 8).

Transcriptome sequencing technique is instrumental in providing a comprehensive and rapid overview of the sequence and expression information of almost all transcripts in a specific cellular or tissue state [35]. Its application in our study was crucial for unraveling the detailed molecular-level antifungal mechanism of AAWE6. The TCA cycle was the most significant pathway for the enrichment of differentially expressed genes, and all the enriched DEGs were downregulated (Fig. 4). The TCA cycle is a general metabolic pathway in aerobic organisms and is mainly distributed in mitochondria [36]. The results were consistent with our hypothesis that AAWE6 disrupts both the structure and function of mitochondria in *T. rubrum*. Importantly, the TCA cycle is also the hub that connects the metabolism of carbohydrates, lipids, and amino acids [37]. The KEGG-enriched pathways in our study also included pyruvate metabolism, fatty acid metabolism, and glycolysis/gluconeogenesis. Although these pathways were less significantly enriched compared to the TCA cycle, their involvement underscores the broader metabolic impact of AAWE6. The observed decrease in glycogen, as indicated in the TEM images, further supports the idea that the antifungal mechanism of AAWE6 centers on inhibiting the TCA cycle. This inhibition, in turn, indirectly affects nutrient metabolism within the fungal cells.

Furthermore, we conducted a series of experiments to validate the mitochondrial function of *T. rubrum* after treatment with AAWE6. RT-qPCR confirmed the downregulation of genes encoding multiple enzymes in the TCA cycle at the genetic level, in agreement with transcriptomic data (Fig. 5). Moreover, molecular docking techniques were used to predict the binding ability of 11 compounds identified from AAWE6 to the dominant targets (PDH, CS, IDH, SDH and MDH) associated with the TCA cycle (Fig. 6). Surprisingly, SDH and MDH were the targets that bound more tightly to all compounds. MDH plays a key metabolic role in the pathway of aerobic energy production and can catalyze the oxidative dehydrogenation of malate to oxaloacetate [38]. In the present study, the inhibition of AAWE6 on MDH in *T. rubrum* was not only significantly concentration-dependent (Fig. 7B) but also exhibited a notable time dependence (Fig. S5). Based on the results of gene expression and molecular docking, MDH may be the key target for AAWE6 to exert its antifungal effect. In addition, the binding energies of eupatilin and jaceosidin (< −8.0 kcal·mol^{-1}) to these targets were significantly lower than that of the other components, and they generated multiple hydrogen (≥ 5) bonds with the preferred binding sites of SDH and MDH. Numerous studies have shown that flavonoids, particularly eupatilin and jaceosidin, are quality markers of *A. argyi* [39, 40]. Currently, reports on the activity of eupatilin and jaceosidin generally focus on their anti-inflammatory, antioxidant, and antitumor activities [41]. Therefore, our study opens new avenues for their application in the treatment of dermatophyte infections.

PA is the final product of the glycolytic pathway, which enables the interconversion of sugars, fats, and amino acids *in vivo* through the acetyl-CoA and TCA cycles [42]. The TCA cycle begins with the condensation of acetyl-CoA and oxaloacetate to form CA [43]. In this study, we observed a decrease in the levels of both PA and CA with increasing concentrations and exposure time to AAWE6 (Figs. 7C and 7D). These results fully confirmed that AAWE6 significantly inhibited the TCA cycle pathway of *T. rubrum*. In addition to the TCA cycle, the ATP synthesis machinery is also an indispensable biochemical reaction for mitochondrial energy metabolism [44]. Previous studies have shown that mitochondrial cristae structure can directly affect the function of the mitochondrial respiratory chain complex and inhibit the synthesis of ATP [45]. Along with the damage to the mitochondrial

crista structure caused by AAWE6, this subfraction also had an inhibitory effect on ATP content and ATPase activity based on the disruption of energy metabolism (Figs. 7E and 7F). The collective evidence from our study demonstrates that the subfraction AAWE6 exerts its antifungal effects against dermatophytes primarily by disrupting mitochondrial morphology and function.

Conclusion

In summary, our research presents compelling evidence that AAWE6, a subfraction derived from the water extract of *A. argyi* and isolated using D101 macroporous resin, exhibits significant antifungal efficacy against prevalent clinical dermatophytes. Through chemical composition analysis and molecular docking studies, we identified eupatilin and jaceosidin as key contributors to AAWE6's antifungal activity. The potential antifungal mechanism of AAWE6 is summarized in three stages: 1) cutting holes in the wall (penetrating the cell membrane and cell wall); 2) attacking the granary (impairing the structure and function of mitochondria); and 3) cell death. Briefly, our study can provide novel insights into the application of *A. argyi* and its subfraction AAWE6 as anti-dermatophytic medicine therapies.

Supporting Information

Supporting information of this paper can be requested by sending E-mails to the corresponding authors.

References

[1] Mei Y, Dai X, Yang W, *et al*. Antifungal activity of chitooligosaccharides against the dermatophyte *Trichophyton rubrum* [J]. *Int J Biol Macromol*, 2015, **77**: 330-335.

[2] Lu Y, Xu T, Xiong L, *et al*. Clinical observation of terbinafine combined with keratolytic gel for the treatment of dermatophyte infection [J]. *Chin J Dermatovenereol Integr Tradit West Med*, 2018, **17**(6): 509-511.

[3] Rodríguez JV, Pérez-Pico AM, Mingorance-Álvarez E, *et al*. Meta-analysis of the antifungal activities of three essential oils as alternative therapies in dermatophytosis infections [J]. *J Appl Microbiol*, 2022, **133**: 241-253.

[4] Huang R, Wang S. Research progress of Chinese herbal medicine against dermatophytes [J]. *Chin J Control Endem Dis*, 2020, **35**: 432-434.

[5] Monod M. Antifungal resistance in dermatophytes: emerging problem and challenge for the medical community [J]. *J Mycol Med*, 2019, **29**(4): 283-284.

[6] Tian J, Ban X, Zeng H, *et al*. *In vitro* and *in vivo* activity of essential oil from dill (*Anethum graveolens* L.) against fungal spoilage of cherry tomatoes [J]. *Food Con*, 2011, **22**: 1992-1999.

[7] Shrestha SK, Garzan A, Garneau-Tsodikova S. Novel alkylated azoles as potent antifungals [J]. *Eur J Med Chem*, 2017, **133**: 309-318.

[8] Li Z, Guo X, Dawuti G, *et al*. Antifungal activity of ellagic acid *in vitro* and *in vivo* [J]. *Phytother Res*, 2015, **29**(7): 1019-1025.

[9] Cantelli BAM, Bitencourt TA, Komoto TT, *et al*. Caffeic acid and licochalcone A interfere with the glyoxylate cycle of *Trichophyton rubrum* [J]. *Biomed Pharmacother*, 2017, **96**: 1389-1394.

[10] Luo N, Jin L, Yang C, *et al*. Antifungal activity and potential mechanism of magnoflorine against *Trichophyton rubrum* [J]. *J Antibiot*, 2020, **74**(3): 206-214.

[11] Lin M, Yuan Z, Hu D, *et al*. Effect of loureirin A against *Candida albicans* biofilms [J]. *Chin J Nat Med*, 2019, **17**(8): 616-623.

[12] Wang Y, Sun Y, Wang J, *et al*. Antifungal activity and action mechanism of the natural product cinnamic acid against *Sclerotinia sclerotiorum* [J]. *Plant Dis*, 2019, **103**(5): 944-950.

[13] Song X, Wen X, He J, *et al*. Phytochemical components and biological activities of *Artemisia argyi* [J]. *J Funct Foods*, 2019, **52**: 648-662.

[14] Lan X, Zhang Y, Zhu L, *et al*. Research progress on chemical constituents from Artemisiae Argyi Folium and their pharmacological activities and quality control [J]. *China J Chin Mater Med*, 2020, **45**(17): 4017-4030.

[15] Guan X, Ge D, Li S, *et al*. Chemical composition and antimicrobial activities of *Artemisia argyi* Lévl. et Vant essential oils extracted by simultaneous distillation-extraction, subcritical extraction and hydrodistillation [J]. *Molecules*, 2019, **24**(3): 483.

[16] Zheng K, Zhong X, Zhang H. Advances in research on constituents and pharmacological effects of *Artemisia argyi* essential oil [J]. *Chin J Exp Tradit Med Formulae*, 2020, **26**: 224-234.

[17] Wang YL. *Toxicological Safety of Artemisia argyi Extract and Its Effect on Immune and Antioxidant Functions in Mice* [D]. Inner Mongolia Agricultural University 2018, Hohhot, Inner Mongolia.

[18] Chen L, Li J, Zhu Y, *et al*. Weed suppression and molecular mechanisms of isochlorogenic acid A isolated from *Artemisia argyi* extract *via* an activity-guided method [J]. *J Agric Food Chem*, 2022, **70**(5): 1494-1506.

[19] Chen C, Long L, Zhang F, *et al*. Antifungal activity, main active components and mechanism of *Curcuma longa* extract against *Fusarium graminearum* [J]. *PLoS ONE*, 2018, **13**(3): e0194284.

[20] Ghannoum M, Chaturvedi V, Diekema D, *et al*. Multilaboratory evaluation of *in vitro* antifungal susceptibility testing of dermatophytes for ME1111 [J]. *J Clin Microbiol*, 2016, **54**: 662-665.

[21] Chen L, Li J, Zhu Y, *et al*. Caffeic acid, an allelochemical in *Artemisia argyi*, inhibits weed growth *via* suppression of mitogen-activated protein kinase signaling pathway and the biosynthesis of gibberellin and phytoalexin [J]. *Front Plant Sci*, 2022, **12**: 802198.

[22] Zhao W, Zhao Z, Ma Y, *et al*. Antifungal activity and preliminary mechanism of pristimerin against *Sclerotinia sclerotiorum* [J]. *Ind Crops Prod*, 2022, **185**: 115124.

[23] Yang S, Liu H, Wei X, *et al*. BrWAX2 plays an essential role in cuticular wax biosynthesis in Chinese cabbage (*Brassica rapa* L. ssp. *pekinensis*) [J]. *Theor Appl Genet*, 2022, **135**(2): 693-707.

[24] Liu X, Liu J, Jiang T, *et al*. Analysis of chemical composition and *in vitro* antidermatophyte activity of ethanol extracts of *Dryopteris fragrans* (L.) Schott [J]. *J Ethnopharmacol*, 2018, **226**: 36-43.

[25] Valarezo E, Flores-Maza P, Cartuche L, *et al*. Phytochemical profile, antimicrobial and antioxidant activities of essential oil extracted from Ecuadorian species *Piper ecuadorense* sodiro [J]. *Nat Prod Res*, 2021, **35**(24): 6014-6019.

[26] Lu H, Jia Y, Peng Y, *et al*. Oxyresveratrol, a stilbene compound from *Morus alba* L. Twig extract active against *Trichophyton rubrum* [J]. *Phytother Res*, 2017, **31**(12): 1842-1848.

[27] Han B, Xin Z, Ma S, *et al*. Comprehensive characterization and identification of antioxidants in Folium Artemisiae Argyi using high-resolution tandem mass spectrometry [J]. *J Chromatogr B*,

2017, **1063**: 84-92.
[28] Lan X, Zhu L, Huang X, *et al*. Study on identification and quantitation of main compounds in Artemisiae Argyi Folium [J]. *Chin Tradit Herb Drugs*, 2021, **52**(24): 7630-7637.
[29] Cortés JCG, Curto MÁ, Carvalho VSD, *et al*. The fungal cell wall as a target for the development of new antifungal therapies [J]. *Biotechnol Adv*, 2019, **37**(6): 107352.
[30] Zeng H, Li T, Tian J, *et al*. TUBP1 protein lead to mitochondria-mediated apoptotic cell death in *Verticillium dahliae* [J]. *Int J Biochem Cell Biol*, 2018, **103**: 35-44.
[31] Randall EB, Hock M, Lopez R, *et al*. Quantitative analysis of mitochondrial ATP synthesis [J]. *Math Biosci*, 2021, **340**: 108646.
[32] Lee HS, Kim Y. Myricetin disturbs the cell wall integrity and increases the membrane permeability of *Candida albicans* [J]. *J Microbiol Biotechnol*, 2022, **32**(1): 37-45.
[33] Sagatova AA. Strategies to better target fungal squalene monooxygenase [J]. *J Fungi*, 2021, **7**(1): 49.
[34] Zhao YG, Codogno P, Zhang Hong. Machinery, regulation and pathophysiological implications of autophagosome maturation [J]. *Nat Rev Mol Cell Biol*, 2021, **22**: 733-750.
[35] Ding H, Fu R, Xie C, *et al*. Transcriptomic profile of human erythroleukemia cells in response to *Sargassum fusiforme* polysaccharide and its structure analysis [J]. *Chin J Nat Med*, 2021, **19**(10): 784-795.
[36] Xu J, Shao X, Li Y, *et al*. Metabolomic analysis and mode of action of metabolites of tea tree oil involved in the suppression of *Botrytis cinerea* [J]. *Front Microbiol*, 2017, **8**: 1017.
[37] Martínez-Reyes I, Chandel NS. Mitochondrial TCA cycle metabolites control physiology and disease [J]. *Nat Commun*, 2020, **11**(1): 102.
[38] Yang S, Liu L, Li D, *et al*. Use of active extracts of poplar buds against *Penicillium italicum* and possible modes of action [J]. *Food Chem*, 2016, **196**: 610-618.
[39] Li S, Zhou S, Yang W, *et al*. Gastro-protective effect of edible plant *Artemisia argyi* in ethanol-induced rats *via* normalizing inflammatory responses and oxidative stress [J]. *J Ethnopharmacol*, 2018, **214**: 207-217.
[40] Zhu Y, Chen L, Wei X, *et al*. Activity screening and evaluation of *Artemisia argyi* in treatment of ulcerative colitis [J]. *Chin Tradit Herb Drugs*, 2021, **52**(16): 4882-4891.
[41] Wang X, Chen L, Fang Y. Advances in pharmacological effect of eupatilin [J]. *Lishizhen Med Mater Med Res*, 2019, **30**(3): 665-668.
[42] Gray LR, Tompkins SC, Taylor EB. Regulation of pyruvate metabolism and human disease [J]. *Cell Mol Life Sci*, 2014, **71**(14): 2577-2604.
[43] Akram M. Citric acid cycle and role of its intermediates in metabolism [J]. *Cell Biochem Biophys*, 2014, **68**(3): 475-478.
[44] Nazaret C, Heiske M, Thurley K, *et al*. Mitochondrial energetic metabolism: a simplified model of TCA cycle with ATP production [J]. *J Theor Biol*, 2009, **258**(3): 455-464.
[45] Cogliati S, Frezza C, Soriano ME, *et al*. Mitochondrial cristae shape determines respiratory chain supercomplexes assembly and respiratory efficiency [J]. *Cell*, 2013, **155**(1): 160-171.

Cite this article as: CHEN Le, ZHU Yunyun, GUO Chaowei, GUO Yujie, ZHAO Lu, MIAO Yuhuan, DU Hongzhi, LIU Dahui. *Artemisia argyi* extract subfraction exerts an antifungal effect against dermatophytes by disrupting mitochondrial morphology and function [J]. *Chin J Nat Med*, 2024, **22**(1): 47-61.

Associate Professor DU Hongzhi, Doctor of Medicine, MA student adviser. He was selected in Hubei Province High-level Talent Program, the Young Elite Scientists Sponsorship Program by China Association of Chinese Medicine, Wuhan Huanghe Talent Program, Hubei University of Chinese Medicine "Xinglin Talent Program" and so on. At present, he is mainly engaged in the pharmacology of Chinese medicine, the development and utilization of Chinese medicine resources. He has published 52 papers as the first author and corresponding author, including 12 of TOP journal papers such as *APSB*, *Food Chem*, *Cell Death Dis*, *JAFC*, and 2 was the ESI highly cited papers. He presided over more than 10 projects of the National Natural Science Foundation, the Provincial Natural Science Foundation and so on. He Applied for 13 patents, edited 1 English e-book, participated in the compilation of 5 textbooks or books, and 3 group standards.

Professor LIU Dahui, Doctor of Agronomy, Postdoctor of Chinese materia medica, Doctoral supervisor. He is the member of the National TCM Standardization Technical Committee, Young Qihuang Scholar of National Administration of Traditional Chinese Medicine, Young and Middle-aged Experts with Outstanding Contributions in Hubei Province. He is the secretary-general of Chinese Medicine Resources and Ecology Committee of Chinese Ecological Society. His research direction is Chinese medicine resources and Chinese medicine ecological agriculture. He has presided over more than 30 research programs, participated in 1 National Science and Technology Progress Awards and 5 first prize of Provincial and Ministerial Science and Technology Progress Awards , and published more than 180 papers as the first author or corresponding author in *PBJ*, *J Agri Food Chem*, *Front Plant Sci*, etc., chief editor of 5 monographs, deputy editor of 5 monographs. Prof. LIU also has authorized more than 20 invention patents, formulate 1 national standard, 2 industry standard, more than 50 group standards.